Cell, Vol. 98, 641–650, September 3, 1999, Copyright ©1999 by Cell Press

Structural Basis for FGF Receptor Dimerization and Activation

Alexander N. Plotnikov,* Joseph Schlessinger,*† Stevan R. Hubbard,*† and Moosa Mohammadi*‡
*Department of Pharmacology
†Skirball Institute of Biomolecular Medicine
New York University School of Medicine
New York, New York 10016

Summary

The crystal structure of FGF2 bound to a naturally occurring variant of FGF receptor 1 (FGFR1) consisting of immunoglobulin-like domains 2 (D2) and 3 (D3) has been determined at 2.8 Å resolution. Two FGF2:FGFR1 complexes form a 2-fold symmetric dimer. Within each complex, FGF2 interacts extensively with D2 and D3 as well as with the linker between the two domains. The dimer is stabilized by interactions between FGF2 and D2 of the adjoining complex and by a direct interaction between D2 of each receptor. A positively charged canyon formed by a cluster of exposed basic residues likely represents the heparin-binding site. A general model for FGF- and heparin-induced FGFR dimerization is inferred from the crystal structure, unifying a wealth of biochemical data.

Introduction

The mammalian fibroblast growth factor (FGF) family consists of at least 18 structurally related polypeptides (FGF1–18) that are expressed in a specific spatial and temporal manner in embryo and adult vertebrates. FGFs play key roles in a wide variety of crucial biological activities that require cell growth, differentiation, migration, and chemotaxis (reviewed by Burgess and Maciag, 1989; Galzie et al., 1997; Naski and Ornitz, 1998). Two classes of cell surface receptors have been identified for FGFs: high-affinity and low-affinity receptors. The four high-affinity receptors, FGFR1–FGFR4, are composed of an extracellular ligand-binding domain that contains three immunoglobulin (Ig)-like domains (D1–D3), a single transmembrane helix, and a cytoplasmic domain that contains protein tyrosine kinase activity (reviewed by Jaye et al., 1992; Johnson and Williams, 1993). The low-affinity FGF receptors are heparin and heparan sulfate–containing proteoglycans (HSPGs) (reviewed by Burgess and Maciag, 1989).

Ligand-induced dimerization is a key event in transmembrane signaling by receptors with tyrosine kinase activity (reviewed by Lemmon and Schlessinger, 1994). Unlike other growth factors (e.g., platelet-derived growth factor [PDGF]), which are dimeric, FGFs are monomeric and are unable by themselves to induce FGFR activation. FGFs function in concert with either soluble or cell surface–bound HSPGs to promote FGFR dimerization, activation, and induction of biological responses (Ornitz et al., 1992; Spivak-Kroizman et al., 1994; Schlessinger et al., 1995). Dimerization of the extracellular domains leads to juxtaposition of the cytoplasmic domains and subsequent transautophosphorylation on tyrosine residues in the cytoplasmic domains. These phosphotyrosine residues either stimulate the intrinsic catalytic activity of the receptor or serve as recruitment sites for downstream signaling proteins (reviewed by Pawson, 1995). Activated FGFRs transmit their signal by recruiting signaling molecules to the tyrosine autophosphorylation site in the carboxy-terminal tail of the receptor (Mohammadi et al., 1992; Peters et al., 1992). In addition, FGFRs tyrosine phosphorylate a family of docking proteins that recruit additional signaling proteins crucial for signal transmission (Kouhara et al., 1997).

FGF–FGFR binding specificity is an essential element in regulation of FGF activity. Each of the four members of the FGFR family binds to a unique subset of FGFs (Ornitz et al., 1996). The overall complexity of the FGF–FGFR system is further increased through alternative splicing of FGFR mRNA (reviewed by Jaye et al., 1992; Johnson and Williams, 1993). Natural FGFR isoforms lacking D1 or both D1 and the acid box, a continuous stretch of acidic residues in the linker between D1 and D2, have been isolated for FGFR1 and FGFR2 and have been shown to retain the full capacity to bind different FGFs (reviewed by Johnson and Williams, 1993). Thus, D2 and D3 are sufficient for FGF binding and for conferring specificity.

An important splicing event occurs in D3 and has been shown to be important in determining ligand binding specificity. The genomic sequence of this region in FGFR1–3 contains two exons (IIIb and IIIc) for the second half of D3 (Johnson et al., 1991; Miki et al., 1991; Avivi et al., 1993). The critical role of the second half of D3 in conferring ligand specificity is best exemplified by the FGFR2/KGFR (keratinocyte growth factor receptor) system. Both FGFR2 and KGFR are encoded by the same gene. In FGFR2, the second half of D3 is encoded by exon IIIc, while in KGFR it is encoded by exon IIIb. Both FGF1 and FGF7 (KGF) bind to KGFR with high affinity, while FGF2 binds poorly to KGFR. In contrast, both FGF1 and FGF2 bind with high affinity to FGFR2, whereas FGF7 does not bind to FGFR2 (Dell and Williams, 1992; Miki et al., 1992; Yayon et al., 1992).

To elucidate the molecular mechanisms underlying FGF–FGFR activation and specificity, we have determined the crystal structure of the extracellular ligand-binding domain of FGFR1 (D2–D3) in complex with FGF2 at 2.8 Å resolution. Although no heparin analog was included in the crystallization conditions, the FGF2–FGFR1 complex forms a noncrystallographic 2-fold dimer. This dimeric structure reveals the mechanism by which FGF and heparin cooperate to promote FGFR dimerization and activation.

Results and Discussion

Structure Determination

A construct encoding Ig-like domains 2 (D2) and 3 (D3) of the extracellular domain of FGFR1, residues 142 to

‡To whom correspondence should be addressed (e-mail: mohammad@saturn.med.nyu.edu).

Table 1. Summary of Crystallographic Analysis

Data Collection Statistics				
Resolution (Å)	Reflections (Total/Unique)	Completeness (%)	R_{sym}[a] (%)	Signal ($\langle I/\sigma I \rangle$)
25.0–2.8	196,126/24,726	99.8 (98.1)[b]	7.2 (25.5)[b]	18.3

Refinement Statistics[c]					
			Root-Mean-Square Deviations		
Resolution (Å)	Reflections	R_{cryst}/R_{free}[d] (%)	Bonds (Å)	Angles (°)	B Factors[e] (Å^2)
25.0–2.8	23,830	24.0/28.4	0.008	1.4	1.7

[a] $R_{sym} = 100 \times \Sigma_{hkl}\Sigma_i |I_i(hkl) - \langle I(hkl)\rangle|/\Sigma_{hkl}\Sigma_i I_i(hkl)$.
[b] Value in parentheses is for the highest resolution shell: 2.9–2.8 Å.
[c] Atomic model: 5,173 protein atoms and 4 SO_4 ions.
[d] $R_{cryst/free} = 100 \times \Sigma_{hkl} ||F_o(hkl)| - |F_c(hkl)||/\Sigma_{hkl} |F_o(hkl)|$, where F_o ($>2\sigma$) and F_c are the observed and calculated structure factors, respectively. Five percent of the reflections were used for calculation of R_{free}.
[e] For bonded protein atoms.

365, was expressed in *Escherichia coli*. This construct (D23) is missing Ig-like domain 1 (D1), the acid box, and the linker between D3 and the transmembrane helix. The boundaries of this construct were chosen based on limited proteolysis experiments, which were performed on the entire extracellular domain of FGFR1, expressed in insect cells, in complex with FGF1. D23 is very similar to a naturally occurring splice variant of FGFR1 that retains full ligand binding capacity (Johnson et al., 1990). When expressed in *E. coli*, D23 was found entirely in inclusion bodies and was solubilized using denaturating reagents and refolded in vitro. Following purification by ion exchange chromatography, D23 was complexed with FGF2 and purified by size exclusion chromatography. The elution position was consistent with the formation of a 1:1 FGF2–D23 complex. Tetragonal crystals of FGF2–D23 were obtained using ammonium sulfate as a precipitating agent. The crystals contain two 1:1 FGF2:D23 complexes in the asymmetric unit, related by an approximate 2-fold axis.

The crystal structure of FGF2–D23 was solved by molecular replacement using FGF2 and telokin as search models (see Experimental Procedures for details). The structure has been refined at 2.8 Å resolution with an R value of 24% (free R value of 28%). The atomic model consists of two FGF2 molecules (residues 16–144), two D23 molecules (residues 149–359), and four sulfate ions. Data collection and refinement statistics are given in Table 1.

Description of the Structure

The dimer in the asymmetric unit of the crystal comprises two 1:1 FGF2–D23 complexes (Figure 1). Within each complex, FGF2 interacts extensively with D2, D3, and the linker between the two domains. The dimeric structure is stabilized by direct receptor–receptor interactions (D2–D2) and interactions between FGF2 and D2 of the other receptor in the dimer. The two FGF2 ligands are on opposite sides of the dimer and are not in contact. As reported previously (Eriksson et al., 1991; Zhang et al., 1991; Zhu et al., 1991), FGF2 adopts a β-trefoil fold that consists of three copies of a four-stranded antiparallel β sheet.

The three-dimensional folds of D2 and D3 place them in the I-set subgroup of the Ig superfamily (reviewed by Williams and Barclay, 1988), as previously predicted on the basis of sequence alignments (Bateman and Chothia, 1995). The fold of D2 can be described as a β barrel formed by two layers of β sheets. One sheet is formed by strands βA, βB/βB′, βE, and βD, and the other by strands βA′, βG, βF, βC, and βC′ (Figure 2A). A disulfide bond between Cys-178, located between βB and βB′, and Cys-230, situated on βF, bridges the two β sheets. This disulfide bond is buried in the hydrophobic core of the domain. The overall strand topology of D2 is similar to that of the canonical I-set member telokin (Holden et al., 1992). Indeed, D2 and telokin can be superimposed (78 common Cα atoms) with a root-mean-square (rms) deviation of only 0.8 Å. Nevertheless, there are significant deviations between D2 and telokin. Strands βA and βE in D2 are shorter than the corresponding strands in telokin. As a result, βB in D2 is discontinuous, consisting of two short strands, βB and βB′. Another difference occurs in the crossover connection between strands βA and βA′. In D2, there is a four-residue insertion vis-à-vis telokin, which forms a 3_{10} helix (helix A) that bulges out from the main body of the domain.

Superposition of D3 with telokin (71 common Cα atoms) also gives an rms deviation of only 0.8 Å. A major difference in topology between D3 and telokin, and also between D3 and D2, occurs after βC. In D3, a large insertion of 14 residues forms an extended loop between βC and βC′ (Figure 2A). This loop is ordered in only one of the two D23 molecules in the asymmetric unit. βC′ is substantially longer in D3 and directs the polypeptide chain toward the upper end of the domain. βD is missing altogether in D3, and in its place is a short α helix (αD). Significantly, this divergent portion of D3 contacts the ligand (see below). The D3 chain reconverges with D2 and telokin at βE. The disulfide bond in the hydrophobic core of D3 is made between Cys-277 and Cys-341.

Primary Interaction Site between FGF2 and FGFR1

FGF2 interacts with residues in D2 and D3 as well as in the linker between D2 and D3 (Figures 3 and 4). These interactions constitute the primary FGF2–FGFR1 interaction site. The interface between the ligand and receptor is extensive, with a total of ~2700 Å^2 of accessible surface area buried. The primary interaction site will be

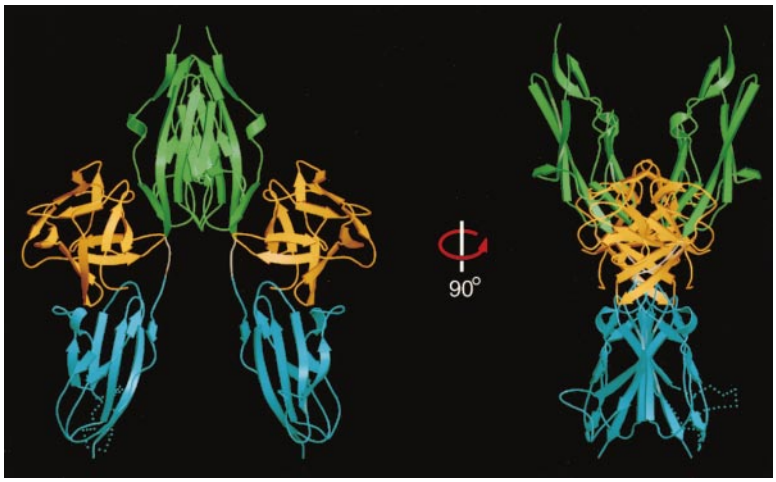

Figure 1. Ribbon Diagram of the Dimeric FGF2–D23 Structure, in Two Views Related by a Rotation of Approximately 90° about the Vertical Axis

The Ig-like domains 2 (D2) and 3 (D3) of the two D23 molecules are shown in green and blue, respectively. The short linker that connects D2 and D3 is colored gray. The two FGF2 molecules are shown in orange. The loop between βC and βC′ is ordered in only one of the two D23 molecules. This loop has been grafted onto the second D23 molecules and indicated as a dotted line. This figure was created using the programs Molscript and Raster3D (Kraulis, 1991; Merrit and Bacon, 1997).

described first with respect to D2, then to the D2–D3 linker, and finally to D3.

Apart from a single hydrogen bond between the side chain of Tyr-24 in FGF2 and the backbone of Leu-165 in FGFR1, hydrophobic interactions dominate the interface between FGF2 and D2 (Figure 5A). The side chains of Tyr-24 and Met-142 of FGF2 are in hydrophobic contact with Ala-167 of D2, and the side chains of Asn-102, Tyr-103, and Leu-140 of FGF2 form a hydrophobic patch with Pro-169 of D2. Ala-167 and Pro-169 are located in βA′ of D2. The aliphatic side chain of Val-248, located in the linker region of FGFR1, interacts with Leu-140 of FGF2 and contributes to the hydrophobicity of FGF2–D2 interface (Figure 5A). Ala-167, Pro-169, and Val-248 of D2 are well conserved among the four mammalian FGFRs (Figure 2B), suggesting that this hydrophobic surface may represent a conserved interaction site for other FGF family members.

The hydrophobic interactions observed in the crystal structure between FGF2 and D2 are in agreement with biochemical studies by Springer et al. (1994), who have mutated solvent-exposed residues of FGF2 based on the unliganded FGF2 crystal structure (Eriksson et al., 1991; Zhang et al., 1991; Zhu et al., 1991) and tested these mutants for FGFR1 binding and mitogenic activity. The binding site, as mapped by Springer et al. (1994), consists primarily of the hydrophobic residues Tyr-24, Tyr-103, Leu-140, and Met-142 of FGF2. Individual substitutions of these hydrophobic residues in FGF2 with alanine resulted in a dramatic decrease (>100-fold) in FGFR1 binding. All four of these hydrophobic residues are found in the FGF2–FGFR1 interface in the present structure.

Ala-167 of FGFR1, which interacts with FGF2, is part of the conserved sequence motif ^{166}HAV^{168} found in FGFRs. This motif is a hallmark of cell adhesion molecules (CAMs) and has been shown to be important for homophilic interactions between CAMs on different cells (Blaschuk et al., 1990; Noe et al., 1999). It has been proposed that neurite outgrowth stimulated by a subset of CAMs is mediated by FGFR activation (Doherty et al., 1995). According to this model, CAMs activate FGFRs by interacting directly with FGFRs via the HAV motif (reviewed by Doherty and Walsh, 1996). However, in the crystal structure, the side chains of His-166 and Val-168 are partially buried in the hydrophobic core of D2 and are clearly important for proper folding of D2. In contrast, in the crystal structure of cadherin (Shapiro et al., 1995), the side chains of the HAV motif are all solvent exposed and poised for homophilic interaction.

The linker between D2 and D3 is highly conserved among the four members of the FGFR family (Figure 2B). Arg-250 in the linker is invariant and is seen in the crystal structure to be directly involved in ligand binding and in interaction with D3. The guanidinium group of Arg-250 makes two hydrogen bonds with FGF2: one with the backbone carbonyl oxygen of Asn-102 and another with the side chain carbonyl oxygen of Asn-104 (Figure 5B). The side chain amide group of Asn-104 in FGF2 is also engaged in an intramolecular hydrogen bond with Tyr-106 of FGF2, which in turn is hydrogen bonded to Glu-96, an invariant residue in the FGF family. The side chain of Glu-96 is hydrogen bonded to the backbone amide nitrogen of Gln-284 in D3 (Figure 5B). The intramolecular FGF hydrogen bonds most likely serve to restrict the conformational freedom of the Asn-104 and Glu-96 side chains, minimizing the entropic cost of receptor binding.

Site-directed mutagenesis studies confirm the importance of these FGF residues in receptor binding. Replacement of Asn-104 by alanine resulted in a >400-fold loss of receptor binding affinity (Zhu et al., 1997), while replacement of Glu-96 with alanine resulted in a 1000-fold reduction (Zhu et al., 1995). Substitution of Tyr-106 with phenylalanine caused a 5-fold reduction in receptor binding (Zhu et al., 1995), indicating that Glu-96 and Asn-104 require intramolecular hydrogen bonds with the side chain of Tyr-106 for the proper positioning of Glu-96 and Asn-104 for receptor interaction.

The side chains of Val-248 in the D2–D3 linker and Leu-98 in FGF2 create a hydrophobic environment for the aliphatic portion of the Arg-250 side chain. Two intramolecular hydrogen bonds between the Arg-250 guanidinium group and the side chain carboxylate group of Asp-282 in D3 (Figure 5B) probably serve to restrict the rotational freedom of the Arg-250 side chain so that it is poised (small entropic loss) to interact with the ligand. Reciprocally, this interaction may also help to orient D3 for optimal interaction with the ligand.

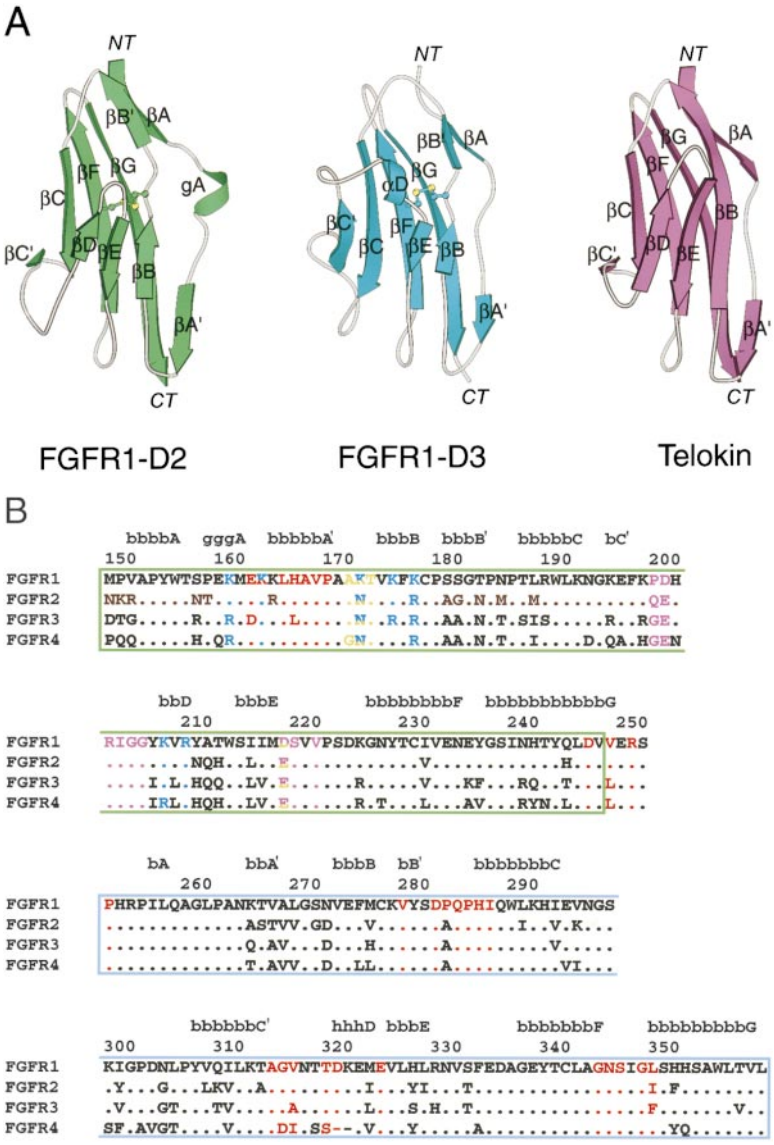

Figure 2. Overall Topology of the Ig-like Domains D2 and D3 of FGFR1 and Sequence Alignment of the Ligand-Binding Domain in the FGFR Family

(A) Comparison of the overall folds of D2 and D3 of FGFR1 with that of the I-set member telokin. The β strands are labeled according to the telokin fold, from A to G. The helix between βA and βA′, gA, is a 3_{10} helix. The cysteines forming the disulfide bridge between the two β sheet layers in D2 and D3 are rendered in ball-and-stick. The amino and carboxyl termini are denoted by NT and CT. This figure was created using the program Molscript.

(B) Structure-based sequence alignment of the ligand-binding domain (D2, D2–D3 linker, and D3) of the four human FGF receptors (FGFR1–4). The secondary structure assignments for FGFR1 were obtained using the Kabsch and Sander algorithm as implemented in PROCHECK (Laskowski et al., 1993). The location and length of the strands and helices are shown on the top of the sequence alignment. The letter "g" denotes a residue in a 3_{10} helix. Only 3_{10} helices comprising four or more residues are indicated. D2 and D3 are demarcated by green and blue boxes, respectively. A period represents sequence identity to FGFR1. FGFR residues involved in direct receptor–receptor interaction are shown in yellow. FGFR residues engaged in the primary FGF2–FGFR1 interaction site are colored red. In blue are FGFR residues that form the sides of the positively charged canyon between the D2 domains in the dimer. FGFR residues participating in the secondary FGF–FGFR interaction site are colored purple. Residues that are engaged in two interaction sites are bicolored.

The interactions between D3 and FGF2 take place at the upper end of D3 (Figures 3 and 4). Many of these interactions involve residues in the segment between βC′ and βE, which is structurally divergent from D2 and other members of the I-set family (Figure 2A). Several regions of FGF2 interact with D3, including the N-terminal segment of FGF2, outside of the β-trefoil core (Figure 5C). The side chain of Phe-17 in FGF2 inserts into a shallow hydrophobic pocket in D3 formed by Pro-285, Ile-287, and the aliphatic portions of the Glu-324 and Asp-320 side chains (Figure 5C). In addition, the backbone of Phe-17 is hydrogen bonded to the Gln-284 side chain. The side chain of Lys-21, another residue in the N-terminal segment of FGF2, forms a hydrogen bond with the side chain of Gln-284 and the backbone of Asp-282 (Figure 5C).

The N-terminal boundary of FGF2, Gly-15, was chosen based on the crystal structure of FGF2 (Faham et al., 1996), in which the first ordered residue is Pro-20. Given that the first ordered residue in the present structure is His-16, it is conceivable that there are additional interactions with D3 involving FGF2 residues N-terminal to Gly-15, the most divergent region in FGFs. The involvement of Phe-17 in receptor binding is supported by inhibition of FGF2 binding to FGFR1 and by inhibition of FGF2-induced proliferation of vascular endothelial cells using a hexapeptide corresponding to FGF2 residues 13–18 that was identified by phage display experiments (Yayon et al., 1993).

Residues 56–60 of FGF2, in β4 and the β4–β5 loop, are in close vicinity to D3 and contribute to ligand binding (see Figure 3). The side chain of Gln-56 makes two hydrogen bonds with Asp-320 in αD of D3, one with the backbone amide nitrogen and another with the side chain carboxylate group (Figure 5C). In addition, the aliphatic portion of the Gln-56 side chain is in van der Waals contact with Gly-315. Ala-57 makes van der Waals contacts with Pro-285 and Gly-315. Glu-58 is hydrogen bonded via its side chain carboxylate group to the backbone amide nitrogen of Val-316 and is also within van der

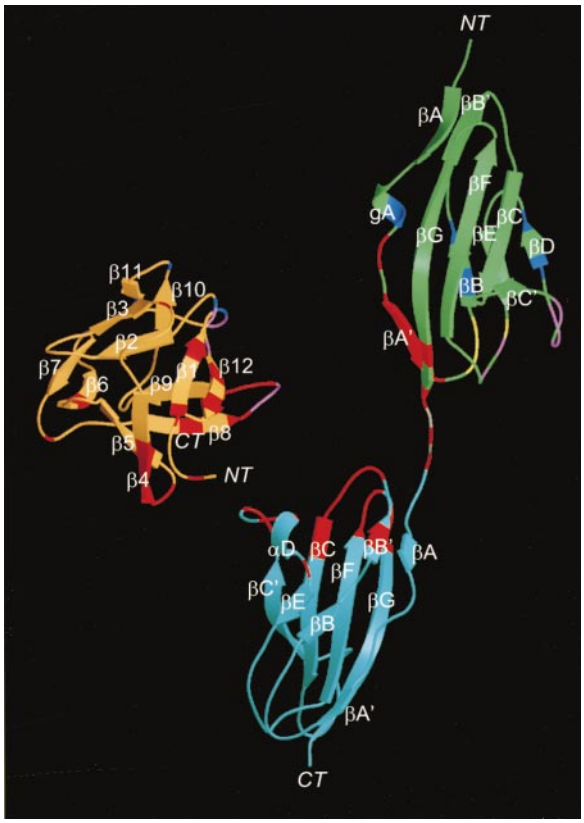

Figure 3. Mapping of the Different Interaction Sites onto the Ribbon Representations of FGF2 and FGFR1

The color codings for D2, D3, the linker, and FGF2 are the same as in Figure 1. The amino and carboxyl termini are denoted by NT and CT. The β strands of FGF2 are labeled from 1 to 12 according to published nomenclature (Faham et al., 1996). Residues of FGF2 and D23 engaged in the primary interaction site are shown in red. FGF2 and D23 residues engaged in the secondary interaction site are colored purple. FGFR1 residues involved in direct receptor–receptor interaction are shown in yellow. Residues of FGF2 known to bind to heparin are shown in blue. Also in blue are FGFR1 residues proposed (based on the present structure) to interact with heparin. In this figure, FGF2 has been pulled away from FGFR1. This figure was created using the programs Molscript and Raster3D.

Waals distance of His-286 and Gly-315. The backbone of Glu-59 is in van der Waals contact with the side chain of His-286. The guanidinium group of Arg-60 is hydrogen bonded to the backbone carbonyl oxygen of Asn-345. This region of FGF2 (residues 56–60) is divergent among the 18 FGF family members, suggesting that these residues may confer FGF–FGFR specificity.

In the absence of ligand, Val-316 of D3, in the βC′–αD loop, would be solvent exposed. However, in the complex, Val-316 is engaged in a hydrophobic interaction with Val-88 of FGF2. Mutagenesis experiments support the involvement of Val-88 in receptor binding. Replacement of Val-88 with alanine in FGF2 causes a 10-fold reduction in receptor binding affinity (Zhu et al., 1998).

The present structure shows why ligand binding and specificity require both D2 and D3 of FGFRs and contradicts reports that suggest D2 of FGFR1 by itself can bind FGFs (Cheon et al., 1994; Wang et al., 1999). This conclusion is also consistent with our in vitro studies demonstrating that FGF1, FGF2, FGF4, and FGF9 are not capable of binding to either D2 or D3 alone (M. M. et al., unpublished results). It is interesting to note that while the interactions between FGF2 and D3 are of both hydrophobic and polar character, hydrophobic contacts dominate the interface between FGF2 and D2.

Ligand–Receptor Interactions that Stabilize Dimerization

The dimer observed in the crystal structure is stabilized by a direct receptor–receptor interaction and by contacts between FGF2 and the other receptor in the dimer, which we designate as the secondary interaction site. These interactions, which are relatively few compared to those in the primary FGF–FGFR interaction site, may aid in FGF- and heparin-induced FGFR dimerization but are presumably not of sufficient strength to allow heparin-independent FGF-induced FGFR dimerization in the context of the native receptor.

The total accessible surface area buried in the secondary interaction site is only 735 Å^2 (Figure 4). Apart from a backbone–backbone hydrogen bond between Pro-132 of FGF2 and Gly-204 of the receptor (in D2), the remainder of the interactions are van der Waals contacts. Residues of FGF2 in the β8–β9 loop (Asp-99, Ser-100, Asn-101) and the β11–β12 loop (Pro-132, Gly-133, Leu-138) are in van der Waals contact with D2 residues in the βC′–βD loop (Pro-199, Asp-200, Ile-203, Gly-204, Gly-205) and the βE–βF loop (Ser-219, Val-221). The side chain of Lys-26 in FGF2 forms a hydrogen bond with the side chain of Asp-218 of D2. Because Lys-26 has been identified as a heparin-binding residue (Faham et al., 1996), the observed interaction with Asp-218 may or may not occur in the presence of heparin. Interestingly, a secondary FGFR1-binding site on FGF2 was identified previously, consisting of Lys-110, Tyr-111, and Trp-114 (Springer et al., 1994). However, these residues are not found in the secondary interaction site in the dimer and, in fact, are quite distant from the receptor.

Superposition of receptor-bound FGF2 with free FGF2 (Zhang et al., 1991) shows that the only significant structural change that occurs upon receptor binding is in the secondary interaction site of FGF2. The β turn containing Ser-100, Asn-101, and Asn-102 undergoes a conformational shift to optimize the interaction with the receptor. Since Asn-101 is a residue in the secondary interaction site and not the primary site, mutation of this residue should not affect formation of the 1:1 FGF2:FGFR1 complex. This is in accord with Zhu et al. (1997) but is contrary to the study by Springer et al. (1994), who reported that replacement of Asn-101 with alanine results in a 7-fold decrease in FGF2 binding to FGFR1. In the crystal structure of FGF2 complexed with a hexasaccharide (Faham et al., 1996), Asn-101 is hydrogen bonded to one of the hexasaccharide sulfate groups and constitutes part of the low-affinity heparin-binding site. The present structure shows that receptor engagement would preclude Asn-101 from contributing to heparin binding.

In general, the ligand–receptor contacts in the secondary interaction site are nonspecific in nature, for example, backbone–backbone van der Waals contacts. Such interactions would allow other ligand–receptor

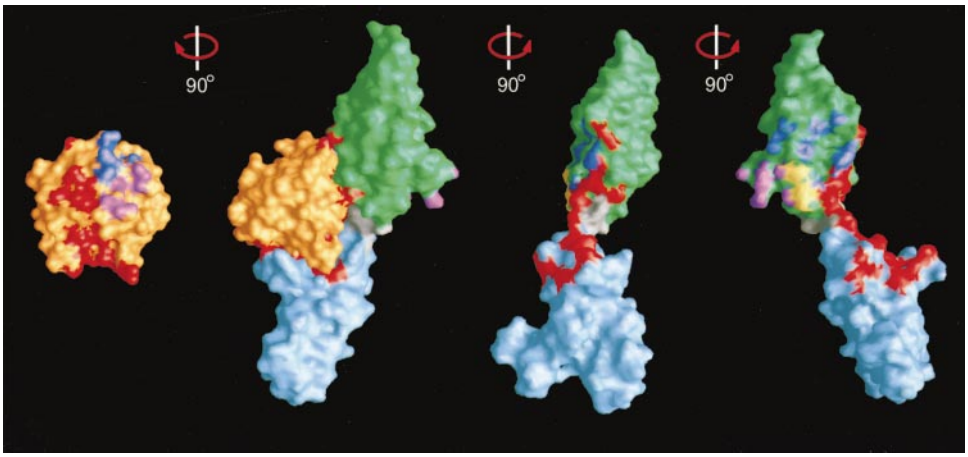

Figure 4. Mapping of the Different Interaction Sites onto the Molecular Surfaces of FGF2 and FGFR1

The surface color codings for D2, D3, the linker, and FGF2 are the same as in Figure 1. The surfaces of FGF2 and FGFR1 that form the primary and secondary interaction sites are shown in red and purple, respectively. The heparin-binding surfaces are depicted in blue. The surface on D2 engaged in direct receptor–receptor interaction is colored yellow. To better visualize the different functional surfaces on FGF2 and D23, the two molecules are pulled away from each other and rotated 90° about the vertical axis. This figure was created using the program GRASP (Nicholls et al., 1991).

combinations to adopt the same dimeric form as observed for FGF2–FGFR1.

Receptor–Receptor Interactions that Stabilize Dimerization

The dimeric structure is also stabilized by a direct receptor–receptor interaction. The interaction between the two FGFR1 molecules in the dimer is limited to a region of D2 at the bottom of the domain, involving residues in the βA′–βB and βE–βF loops (Figure 3). The total surface area buried at this interface is only ~300 Å^2 (Figure 4). Across the 2-fold axis of the dimer, the Ala-171 side chain makes a hydrophobic contact with the Ala-171 side chain from the other receptor. Main chain atoms of Ala-171 and Lys-172 are in van der Waals contact with the corresponding atoms in the adjacent receptor. Hydrogen bonds between the side chain of Thr-173 and the backbone nitrogen of Thr-173 of the other receptor and between the side chains of Lys-172 and Asp-218 fortify the interface.

Sequence conservation in this region of D2 among FGFRs is consistent with this region forming a receptor–receptor interface. The residue at the closest approach in the dimer interface is Ala-171, which is conserved in FGFR1–3 and replaced by glycine in FGFR4 (Figure 2B). In addition, the hydrogen-bonding potential at the interface is conserved in FGFR2-4. Asp-218 and Lys-172 in FGFR1 are replaced by potential hydrogen-bonding partners glutamic acid and asparagine, respectively, in FGFR2-4. Thr-173 is conserved in all four FGFRs (Figure 2B). Intriguingly, the interactions observed at the receptor–receptor interface are compatible with FGFR heterodimerization, which has been detected in transfected cell lines expressing FGFR1 and FGFR2 (Bellot et al., 1991). A role for direct receptor–receptor interaction in FGFR dimerization has been postulated previously (Pantoliano et al., 1994; Wang et al., 1997). However, the observed receptor–receptor interface in the crystal structure differs from those previously proposed.

The Proposed Heparin-Binding Canyon

Calculation of the electrostatic potential at the surface of the dimer reveals a highly positive "canyon" whose sides are the inward faces of D2 from the two receptors in the dimer (Figure 6B). The positive potential continues onto the top side of the two ligands on either side of the canyon. The positive potential in the canyon is provided primarily by the lysines that constitute the heparin-binding site on D2 (Kan et al., 1993; Figure 6A). These lysines are located in an 18-residue stretch from helix A through βB and include Lys-160, Lys-163, Lys-172, Lys-175, and Lys-177. Although Lys-164 is contained in this region, it is located on the outward face of D2. We propose that this canyon is the site of heparin binding.

While the side chains of Lys-160, Lys-175, and Lys-177 are disordered (probably due to the lack of heparin), the side chains of Lys-163 and Lys-172 are ordered and chelate a sulfate ion located in the canyon at the junction between the ligand and receptor. The same sulfate ion is also chelated by Lys-26 and Lys-135 from the ligand. Based on the crystal structure of FGF2 complexed with a hexasaccharide (Faham et al., 1996), these two lysines were assigned to the low-affinity heparin-binding site. This observed sulfate-mediated ligand–receptor interaction may explain in part why heparin increases the apparent affinity of FGF2 for FGFR1 (Roghani et al., 1994).

The high-affinity heparin-binding site on FGF2 consists of Asn-27, Lys-125, Gln-134, and Arg-120 (Faham et al., 1996). These residues are located on the top surface of FGF2 adjacent to the end of the canyon. An ordered sulfate ion is bound in the high-affinity heparin-binding site of each of the two FGF2 molecules in the dimer (Figure 6A). In addition to the modeled sulfate ions, there are several positive peaks in the difference electron density map within the canyon that are likely to represent partially ordered sulfate ions. In the absence of heparin, the sulfate ions are probably important for neutralizing the many positively charged residues

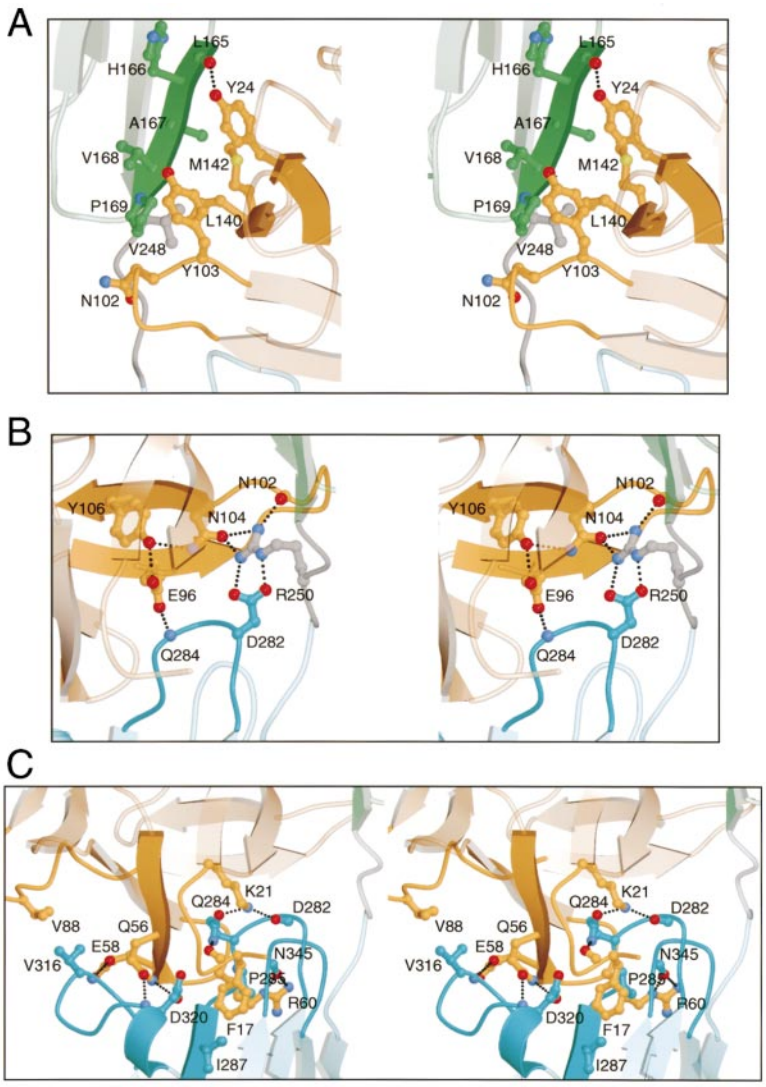

Figure 5. The Primary Interaction Site between FGF2 and FGFR1

(A) Stereo view of the hydrophobic interface between FGF2 and D2 of FGFR1. Only side chains of interacting residues are shown. Color coding is the same as in Figure 1: FGF2 in orange, D2 in green, D3 in blue, and the linker in gray. Dotted lines represent hydrogen bonds.

(B) Stereo view of the network of hydrogen bonds between FGF2 and FGFR1 in the vicinity of Arg-250 in the D2–D3 linker.

(C) Stereo view of the interface between FGF2 and D3 of FGFR1. This figure was created using the programs Molscript and Raster3D.

of D2 in the canyon, allowing formation of the dimer. Moreover, the sulfate ions most likely demarcate the path of a bound heparin molecule, which would traverse the canyon and interact with the heparin-binding sites on the receptors and the ligands at the ends of the canyon.

The hypothesis that the canyon represents the site of heparin binding is further supported by biochemical studies aimed at determining the minimal length of heparin necessary for FGF signaling (Ornitz et al., 1992). The results indicate that the shortest biologically active heparin oligosaccharide is an octasaccharide and that an increase in activity parallels an increase in heparin length up to a dodecasaccharide, at which point the activity plateaus. Manual docking of a hexasaccharide, which is not biologically active, into the dimer canyon demonstrates that while the hexasaccharide can interact with the heparin-binding site on the receptor, it is not long enough to reach the heparin-binding site on the ligands. In contrast, an octasaccharide placed into the canyon is able to reach the low-affinity heparin-binding site on the two ligands. A longer oligosaccharide such as a dodecasaccharide could engage residues in both the low- and high-affinity sites on the two ligands (Figure 6B).

The crystal structure suggests that other basic residues of D2 that point into the canyon may also be involved in heparin binding, although they have not been implicated previously. Lys-207 and Arg-209 are situated at the top of the canyon in βD. Lys-207 is conserved in FGFR1–3, and an arginine is present at this position in FGFR4. Arg-209 is conserved in all four FGFRs (Figure 2B). Interestingly, Ala-211, which is nearby and also points into the canyon, is a glutamine in FGFR2-4, a residue that can form a hydrogen bond with the sulfate groups of heparin. It is likely that sequence differences in the heparin-binding region in FGFRs modulate the affinity and specificity for glycosaminoglycans, which are naturally heterogeneous in carbohydrate sequence and sulfation.

Conclusions

The dimeric FGF:FGFR structure described in this report reveals a detailed view of how a growth factor binds to a naturally occurring variant of an extracellular domain

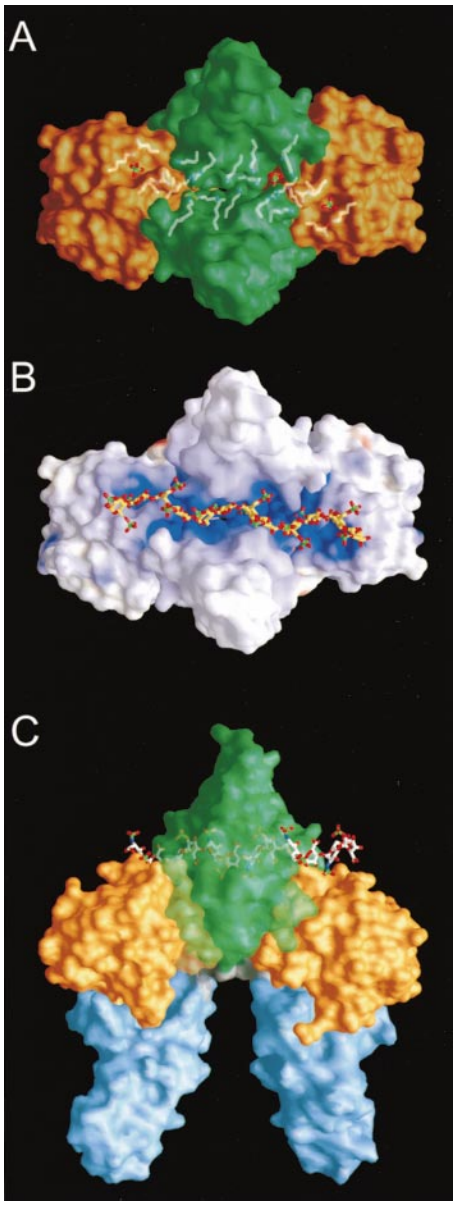

Figure 6. The Putative Heparin-Binding Canyon

(A) Molecular surface representation of the dimeric FGF2–FGFR1 complex. The view is from the top (with respect to the left panel in Figure 1) looking down into the proposed heparin-binding canyon. The surface coloring is the same as in Figure 4, with FGF2 in orange and D2 in green. The side chains of the identified or proposed heparin-binding residues on D2 and the identified low- and high-affinity heparin-binding sites in FGF2 are rendered in ball-and-stick. The ordered sulfate ions in the high-affinity heparin-binding site on FGF2 and in the canyon at the junction between FGF2 and D2 are shown. (B) Surface charge distribution of the dimeric FGF2–FGFR1 complex. The view is the same as in (A). Blue and red represent positive and negative electrostatic potential, respectively. Side chains of lysine, arginine, glutamic acid, and aspartic acid that are disordered but would point into the canyon were manually positioned. The positively charged canyon runs between the two D2 domains of the receptors in the dimer and extends across the adjoining ligands. The positive potential of the surface is provided by the putative heparin-binding residues on D2 and the low- and high-affinity heparin-binding sites on FGF2. A heparin dodecasaccharide is docked manually into the proposed heparin-binding site. This figure was created with GRASP.

of a receptor tyrosine kinase, leading to receptor dimerization and activation. In addition, the salient features of this structure enable the interpretation of a large body of work describing the binding characteristics of FGF and FGFR mutants, as well as how heparin in concert with FGF induces FGFR dimerization and activation. We conclude that multiple binding events contribute toward the generation of a stable FGF:FGFR dimeric complex. The present crystal structure reconciles the ability of heparin to both induce dimerization of FGF and interact with the heparin-binding region on FGFRs. A positively charged canyon is formed between the two D2 domains of FGFRs and extends onto the heparin-binding sites on the ligands. We propose that this canyon represents the heparin-binding site. In this model, FGF interacts with both receptor molecules within the dimer through primary and secondary sites. The direct receptor–receptor interactions observed in our structure are confined to a small interface located in D2 at the bottom of the heparin-binding canyon. Both the direct receptor–receptor interactions and the interaction of FGF2 with the adjoining receptor contribute toward stabilization of the dimeric structure. There are no direct interactions between the two FGF molecules (Figure 6C).

The dimeric model deduced from the crystal structure also affords a possible role for the acid box, a continuous stretch of acidic residues in the linker between D1 and D2. Modeling experiments show that the acid box has the potential to interact with the basic heparin-binding region on D2, especially since the linker between the acid box and the beginning of D2 is long enough to allow this interaction to occur. The model inferred from the crystal structure implies that binding of heparin (in the absence of FGF) to the heparin-binding surfaces on D2 could cause FGF-independent dimerization of FGFRs. Indeed, heparin-induced FGF-independent activation of FGFR4 has been described (Gao and Goldfarb, 1995). We surmise that in the context of the full-length receptor, the acid box is bound to the basic heparin-binding region on D2, thereby competing with heparin for FGFR binding. This autoinhibition would prevent FGF-independent activation of FGFR by heparin sulfate proteoglycans that are found in abundance on the surface of most cell types. Interaction of the acid box with the heparin-binding region on D2 could also enable D1 to fold over onto D2 and D3 and affect the interaction with FGF. This hypothesis is consistent with studies demonstrating that an FGFR1 deletion mutant lacking D1 and the acid box exhibits higher binding affinity for FGF and heparin (Wang et al., 1995). Interestingly, progression of human pancreatic and brain tumors toward malignancy has been correlated with a switch in alternative splicing of FGFRs leading to expression of FGFRs missing D1 and the acid box (Kobrin et al., 1993; Yamaguchi et al., 1994).

(C) Molecular surface view of the dimeric FGF2–FGFR1 complex with a heparin dodecasaccharide docked manually into the proposed heparin-binding site. Coloring and viewing angle are the same as in Figure 1. The dodecasaccharide is sandwiched (*trans*) between the D2 domains of the receptor monomers and interacts at both ends with the FGF2 molecules in a *cis* manner. To see the path of the dodecasaccharide, the front D2 was made semitransparent. This figure was prepared with GRASP.

Although it is well established that receptor dimerization is essential for transmission of signals across the plasma membrane, it has been less clear whether dimerization is sufficient or whether higher oligomerization states are required in signal transmission. This question is particularly valid in the FGF–FGFR system, since heparin can bind simultaneously to numerous FGF molecules (Schlessinger et al., 1995). An intriguing outcome of the model derived from the crystal structure is that dimerization should be sufficient for activation of FGFR and signal transduction across the plasma membrane. Docking of various oligosaccharides into the positively charged canyon shows that a dodecasaccharide, the optimal biologically active heparin analog, perfectly transverses the entire length of the canyon and engages both the low- and high-affinity heparin-binding sites on the FGF2 molecules. Since a dodecasaccharide is not long enough to bridge two dimeric FGF:FGFR units, it is reasonable to suggest that the dimeric FGF:FGFR structure as observed in the crystal structure may represent the minimal structural unit required for activation of FGFRs.

Experimental Procedures

Crystallization and Data Collection

Crystals were grown by vapor diffusion at 20°C using the hanging drop method. Crystallization buffer containing 1.6 M ammonium sulfate, 20% glycerol, and 0.1 M Tris-HCl (pH 8.5) was mixed in equal volume with protein solution (10 mg/ml, 25 mM Tris-HCl [pH 8.5], 150 mM NaCl). The crystals belong to the tetragonal space group $P4_12_12$, with unit cell dimensions $a = b = 98.5$ Å, $c = 197.0$ Å. There are two molecules of FGF2 and two molecules of D23 in the asymmetric unit with a solvent content of ~58%. A 2.8 Å data set was collected from a flash-frozen (in a dry nitrogen stream) crystal on a CCD detector at beamline X-4A at the National Synchrotron Light Source, Brookhaven National Laboratory. All data were processed using DENZO and SCALEPACK (Otwinowski, 1993).

Structure Determination and Refinement

The structure was determined by molecular replacement using the program AMoRe (Navaza, 1994) and the structures of FGF2 (2FGF [Zhang et al., 1991]) and telokin (1TLK [Holden et al., 1992]) as search models. Homology models for D2 and D3 of FGFR1 were constructed from the telokin structure. A molecular replacement solution was found for two copies of FGF2 and one copy of D2 and D3. The second copy of D2 and D3 was obtained by rigid-body rotation and translation of the first copy onto the second FGF molecule. The placement of the second copy of D2 and D3 was confirmed by rigid-body refinement in CNS (Brünger et al., 1998). Simulated annealing and positional/B factor refinement were performed using CNS. Bulk solvent and anisotropic B factor corrections were applied. Tight noncrystallographic symmetry restraints were imposed throughout the refinement for the backbone atoms of FGF2, D2, and D3. The rms deviation for Cα atoms between the two copies of FGF2, D2, or D3 is 0.04 Å. Model building into $2F_o-F_c$ and F_o-F_c electron density maps was performed with O (Jones et al., 1991). The atomic model includes FGF2 residues 16–144 and FGFR1 residues 149–359, except in one of the FGFR1 copies, where residues 293–307 are disordered. The average B factor is 38.7 $Å^2$ for all atoms, 37.6/38.9 $Å^2$ for FGF2, and 38.3/39.1 $Å^2$ for FGFR1.

Acknowledgments

We thank A. V. Eliseenkova for production of the FGF2 and D23 in *E. coli*; C. Ogata for synchrotron beamline assistance; and J. Till for manuscript comments. S. R. H. is a recipient of a Kimmel Scholar Award from the Sidney Kimmel Foundation for Cancer Research. Beamline X-4A at the National Synchrotron Light Source, a DOE facility, is supported by the Howard Hughes Medical Institute.

Received July 12, 1999; revised August 10, 1999.

References

Avivi, A., Yayon, A., and Givol, D. (1993). A novel form of FGF receptor-3 using an alternative exon in the immunoglobulin domain III. FEBS Lett. *330*, 249–252.

Bateman, A., and Chothia, C. (1995). Outline structures for the extracellular domains of the fibroblast growth factor receptors. Nat. Struct. Biol. *2*, 1068–1074.

Bellot, F., Crumley, G., Kaplow, J.M., Schlessinger, J., Jaye, M., and Dionne, C.A. (1991). Ligand-induced transphosphorylation between different FGF receptors. EMBO J. *10*, 2849–2854.

Blaschuk, O.W., Sullivan, R., David, S., and Pouliot, Y. (1990). Identification of a cadherin cell adhesion recognition sequence. Dev. Biol. *139*, 227–229.

Brünger, A.T., Adams, P.D., Clore, G.M., DeLano, W.L., Gros, P., Grosse-Kunstleve, R.W., Jiang, J.S., Kuszewski, J., Nigles, M., Pannu, N.S., et al. (1998). Crystallography and NMR system: a new software suite for macromolecular structure determination. Acta. Crystallogr. D *54*, 905–921.

Burgess, W.H., and Maciag, T. (1989). The heparin-binding (fibroblast) growth factor family of proteins. Annu. Rev. Biochem. *58*, 575–606.

Cheon, H.G., LaRochelle, W.J., Bottaro, D.P., Burgess, W.H., and Aaronson, S.A. (1994). High-affinity binding sites for related fibroblast growth factor ligands reside within different receptor immunoglobulin-like domains. Proc. Natl. Acad. Sci. USA *91*, 989–993.

Dell, K.R., and Williams, L.T. (1992). A novel form of fibroblast growth factor receptor 2. Alternative splicing of the third immunoglobulin-like domain confers ligand binding specificity. J. Biol. Chem. *267*, 21225–21229.

Doherty, P., and Walsh, F.S. (1996). CAM-FGF receptor interactions: a model for axonal growth. Mol. Cell. Neurosci. *8*, 99–111.

Doherty, P., Williams, E., and Walsh, F.S. (1995). A soluble chimeric form of the L1 glycoprotein stimulates neurite outgrowth. Neuron *14*, 57–66.

Eriksson, A.E., Cousens, L.S., Weaver, L.H., and Matthews, B.W. (1991). Three-dimensional structure of human basic fibroblast growth factor. Proc. Natl. Acad. Sci. USA *88*, 3441–3445.

Faham, S., Hileman, R.E., Fromm, J.R., Linhardt, R.J., and Rees, D.C. (1996). Heparin structure and interactions with basic fibroblast growth factor. Science *271*, 1116–1120.

Galzie, Z., Kinsella, A.R., and Smith, J.A. (1997). Fibroblast growth factors and their receptors. Biochem. Cell. Biol. *75*, 669–685.

Gao, G., and Goldfarb, M. (1995). Heparin can activate a receptor tyrosine kinase. EMBO J. *14*, 2183–2190.

Holden, H.M., Ito, M., Hartshorne, D.J., and Rayment, I. (1992). X-ray structure determination of telokin, the C-terminal domain of myosin light chain kinase, at 2.8 Å resolution. J. Mol. Biol. *227*, 840–851.

Jaye, M., Schlessinger, J., and Dionne, C.A. (1992). Fibroblast growth factor receptor tyrosine kinases: molecular analysis and signal transduction. Biochim. Biophys. Acta *1135*, 185–199.

Johnson, D.E., and Williams, L.T. (1993). Structural and functional diversity in the FGF receptor multigene family. Adv. Cancer Res. *60*, 1–41.

Johnson, D.E., Lee, P.L., Lu, J., and Williams, L.T. (1990). Diverse forms of a receptor for acidic and basic fibroblast growth factors. Mol. Cell. Biol. *10*, 4728–4736.

Johnson, D.E., Lu, J., Chen, H., Werner, S., and Williams, L.T. (1991). The human fibroblast growth factor receptor genes: a common structural arrangement underlies the mechanisms for generating receptor forms that differ in their third immunoglobulin domain. Mol. Cell. Biol. *11*, 4627–4634.

Jones, T.A., Zou, J.Y., Cowan, S.W., and Kjeldgaard, M. (1991). Improved methods for binding protein models in electron density maps and the location of errors in these models. Acta Crystallogr. A *47*, 110–119.

Kan, M., Wang, F., Xu, J., Crabb, J.W., Hou, J., and McKeehan, W.L. (1993). An essential heparin-binding domain in the fibroblast growth factor receptor kinase. Science *259*, 1918–1921.

Kobrin, M.S., Yamanaka, Y., Friess, H., Lopez, M.E., and Korc, M.

(1993). Aberrant expression of type I fibroblast growth factor receptor in human pancreatic adenocarcinomas. Cancer Res. *53*, 4741–4744.

Kouhara, H., Hadari, Y.R., Spivak-Kroizman, T., Schilling, J., Bar-Sagi, D., Lax, I., and Schlessinger, J. (1997). A lipid-anchored Grb2-binding protein that links FGF-receptor activation to the Ras/MAPK signaling pathway. Cell *89*, 693–702.

Kraulis, P.J. (1991). MOLSCRIPT: a program to produce both detailed and schematic plots of protein structures. J. Appl. Crystallogr. *24*, 946–950.

Laskowski, R.A., MacArthur, M.W., Moss, D.S., and Thornton, J.M. (1993). PROCHECK: a program to check the stereochemical quality of protein structures. J. Appl. Crystallogr. *26*, 283–291.

Lemmon, M.A., and Schlessinger, J. (1994). Regulation of signal transduction and signal diversity by receptor oligomerization. Trends Biochem. Sci. *19*, 459–463.

Merrit, E.A., and Bacon, D.J. (1997). Raster3D: photorealistic molecular graphics. Methods Enzymol. *277*, 505–524.

Miki, T., Fleming, T.P., Bottaro, D.P., Rubin, J.S., Ron, D., and Aaronson, S.A. (1991). Expression cDNA cloning of the KGF receptor by creation of a transforming autocrine loop. Science *251*, 72–75.

Miki, T., Bottaro, D.P., Fleming, T.P., Smith, C.L., Burgess, W.H., Chan, A.M., and Aaronson, S.A. (1992). Determination of ligand-binding specificity by alternative splicing: two distinct growth factor receptors encoded by a single gene. Proc. Natl. Acad. Sci. USA *89*, 246–250.

Mohammadi, M., Dionne, C.A., Li, W., Li, N., Spivak, T., Honegger, A.M., Jaye, M., and Schlessinger, J. (1992). Point mutation in FGF receptor eliminates phosphatidylinositol hydrolysis without affecting mitogenesis. Nature *358*, 681–684.

Naski, M.C., and Ornitz, D.M. (1998). FGF signaling in skeletal development. Front Biosci. *3*, D781–D794.

Navaza, J. (1994). AMoRe: an automated package for molecular replacement. Acta Crystallogr. A *50*, 157–163.

Nicholls, A., Sharp, K.A., and Honig, B. (1991). Protein folding and association: insights from interfacial and thermodynamic properties of hydrocarbons. Proteins *11*, 281–296.

Noe, V., Willems, J., Vandekerckhove, J., Roy, F.V., Bruyneel, E., and Mareel, M. (1999). Inhibition of adhesion and induction of epithelial cell invasion by HAV-containing E-cadherin-specific peptides. J. Cell Sci. *112*, 127–135.

Ornitz, D.M., Yayon, A., Flanagan, J.G., Svahn, C.M., Levi, E., and Leder, P. (1992). Heparin is required for cell-free binding of bFGF to a soluble receptor and for mitogenesis in whole cells. Mol. Cell. Biol. *12*, 240–247.

Ornitz, D.M., Xu, J., Colvin, J.S., McEwen, D.G., MacArthur, C.A., Coulier, F., Gao, G., and Goldfarb, M. (1996). Receptor specificity of the fibroblast growth factor family. J. Biol. Chem. *271*, 15292–15297.

Otwinowski, Z. (1993). Oscillation data reduction program. In Proceedings of the CCP4 Study Weekend, L. Sawyer, N. Isaacs, and S. Burley, eds. (Daresbury, UK: SERC Daresbury Laboratory).

Pantoliano, M.W., Horlick, R.A., Springer, B.A., Van Dyk, D.E., Tobery, T., Wetmore, D.R., Lear, J.D., Nahapetian, A.T., Bradley, J.D., and Sisk, W.P. (1994). Multivalent ligand-receptor binding interactions in the fibroblast growth factor system produce a cooperative growth factor and heparin mechanism for receptor dimerization. Biochemistry *33*, 10229–10248.

Pawson, T. (1995). Protein modules and signaling networks. Nature *373*, 573–580.

Peters, K.G., Marie, J., Wilson, E., Ives, H.E., Escobedo, J., Del Rosario, M., Mirda, D., and Williams, L.T. (1992). Point mutation of an FGF receptor abolishes phosphatidylinositol turnover and Ca^{2+} but not mitogenesis. Nature *358*, 678–681.

Roghani, M., Mansukhani, A., Dell'Era, P., Bellosta, P., Basilico, C., Rifkin, D.B., and Moscatelli, D. (1994). Heparin increases the affinity of basic fibroblast growth factor for its receptor but is not required for binding. J. Biol. Chem. *269*, 3976–3984.

Schlessinger, J., Lax, I., and Lemmon, M. (1995). Regulation of growth factor activation by proteoglycans: what is the role of the low affinity receptors? Cell *83*, 357–360.

Shapiro, L., Fannon, A.M., Kwong, P.D., Thompson, A., Lehmann, M.S., Grubel, G., Legrand, J.F., Als-Nielsen, J., Colman, D.R., and Hendrickson, W.A. (1995). Structural basis of cell-cell adhesion by cadherins. Nature *374*, 327–337.

Spivak-Kroizman, T., Lemmon, M.A., Dikic, I., Ladbury, J.E., Pinchasi, D., Huang, J., Jaye, M., Crumley, G., Schlessinger, J., and Lax, I. (1994). Heparin-induced oligomerization of FGF molecules is responsible for FGF receptor dimerization, activation, and cell proliferation. Cell *79*, 1015–1024.

Springer, B.A., Pantoliano, M.W., Barbera, F.A., Gunyuzlu, P.L., Thompson, L.D., Herblin, W.F., Rosenfeld, S.A., and Book, G.W. (1994). Identification and concerted function of two receptor binding surfaces on basic fibroblast growth factor required for mitogenesis. J. Biol. Chem. *269*, 26879–26884.

Wang, F., Kan, M., Yan, G., Xu, J., and McKeehan, W.L. (1995). Alternately spliced NH2-terminal immunoglobulin-like loop I in the ectodomain of the fibroblast growth factor (FGF) receptor 1 lowers affinity for both heparin and FGF-1. J. Biol. Chem. *270*, 10231–10235.

Wang, F., Kan, M., McKeehan, K., Jang, J.H., Feng, S., and McKeehan, W.L. (1997). A homeo-interaction sequence in the ectodomain of the fibroblast growth factor receptor. J. Biol. Chem. *272*, 23887–23895.

Wang, F., Lu, W., McKeehan, K., Mohamedali, K., Gabriel, J.L., Kan, M., and McKeehan, W.L. (1999). Common and specific determinants for fibroblast growth factors in the ectodomain of the receptor kinase complex. Biochemistry *38*, 160–171.

Williams, A.F., and Barclay, A.N. (1988). The immunoglobulin superfamily—domains for cell surface recognition. Annu. Rev. Immunol. *6*, 381–405.

Yamaguchi, F., Saya, H., Bruner, J.M., and Morrison, R.S. (1994). Differential expression of two fibroblast growth factor-receptor genes is associated with malignant progression in human astrocytomas. Proc. Natl. Acad. Sci. USA *91*, 484–488.

Yayon, A., Zimmer, Y., Shen, G.H., Avivi, A., Yarden, Y., and Givol, D. (1992). A confined variable region confers ligand specificity on fibroblast growth factor receptors: implications for the origin of the immunoglobulin fold. EMBO J. *11*, 1885–1890.

Yayon, A., Aviezer, D., Safran, M., Gross, J.L., Heldman, Y., Cabilly, S., Givol, D., and Katchalski-Katzir, E. (1993). Isolation of peptides that inhibit binding of basic fibroblast growth factor to its receptor from a random phage-epitope library. Proc. Natl. Acad. Sci. USA *90*, 10643–10647.

Zhang, J.D., Cousens, L.S., Barr, P.J., and Sprang, S.R. (1991). Three-dimensional structure of human basic fibroblast growth factor, a structural homolog of interleukin 1 beta. Proc. Natl. Acad. Sci. USA *88*, 3446–3450.

Zhu, X., Komiya, H., Chirino, A., Faham, S., Fox, G.M., Arakawa, T., Hsu, B.T., and Rees, D.C. (1991). Three-dimensional structures of acidic and basic fibroblast growth factors. Science *251*, 90–93.

Zhu, H., Ramnarayan, K., Anchin, J., Miao, W.Y., Sereno, A., Millman, L., Zheng, J., Balaji, V.N., and Wolff, M.E. (1995). Glu-96 of basic fibroblast growth factor is essential for high affinity receptor binding. Identification by structure-based site-directed mutagenesis. J. Biol. Chem. *270*, 21869–21874.

Zhu, H., Anchin, J., Ramnarayan, K., Zheng, J., Kawai, T., Mong, S., and Wolff, M.E. (1997). Analysis of high-affinity binding determinants in the receptor binding epitope of basic fibroblast growth factor. Protein Eng. *10*, 417–421.

Zhu, H., Ramnarayan, K., Menzel, P., Miao, Y., Zheng, J., and Mong, S. (1998). Identification of two new hydrophobic residues on basic fibroblast growth factor important for fibroblast growth factor receptor binding. Protein Eng. *11*, 937–940.

Protein Data Bank ID Code

The structure reported in this paper has been deposited in the Protein Data Bank under ID code 1CVS.